Neuron

Supplemental Information

Comprehensive Characterization of the Major Presynaptic Elements to the *Drosophila* OFF Motion Detector

Etienne Serbe, Matthias Meier, Aljoscha Leonhardt, and Alexander Borst

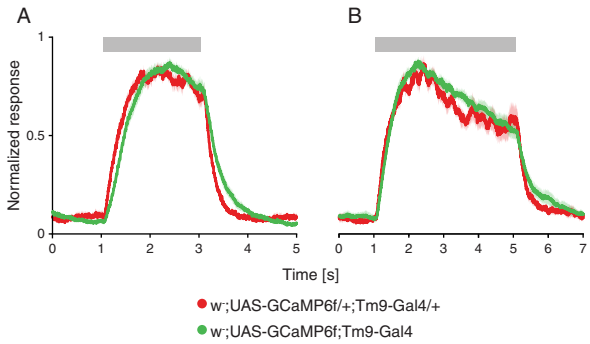

Figure S1. Related to Figure 3. Different expression levels of GCaMP do not affect the response kinetics of Tm9

(A and B) Normalized line scan calcium responses in Tm9 axonal arbors upon stimulation with a 4.5˚ wide, dark bar appearing for 2s (A) and 4s (B) to investigate long term temporal dynamics of Tm9 responses. To exclude effects of GCaMP6f expression level on the dynamics of the response, two traces were obtained using flies with homozygous (green) and heterozygous (red) expression of the Gal4 and the UAS construct. Error shades indicate ±SEM.

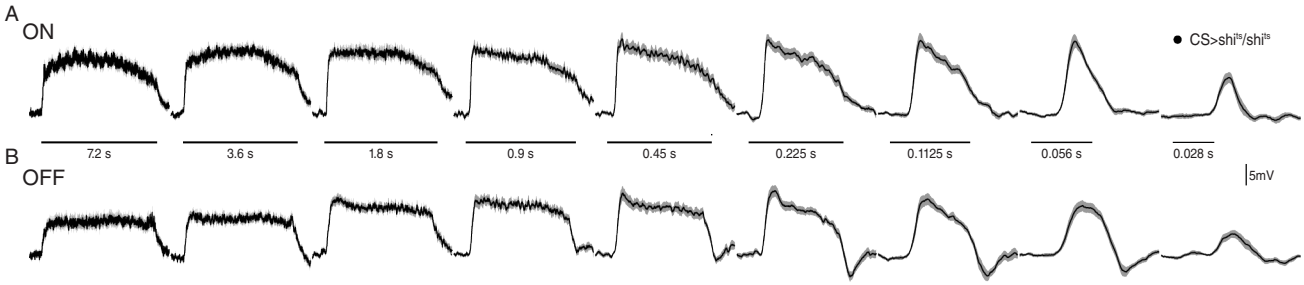

Figure S2. Related to Figure 5. LPTC responses to multiple edges moving at different velocities
Average voltage traces of lobula plate tangential cells in control flies (N=5, n=13), stimulated with multiple moving ON (A) and OFF (B) edges at 9 different velocities (3.125˚/s, 6.25˚/s, 12.5˚/s, 25˚/s, 50˚/s, 100˚/s, 200˚/s, 400˚/s, and 800˚/s). Black bars indicate duration of stimulus presentation. Error shades indicate ± SEM.

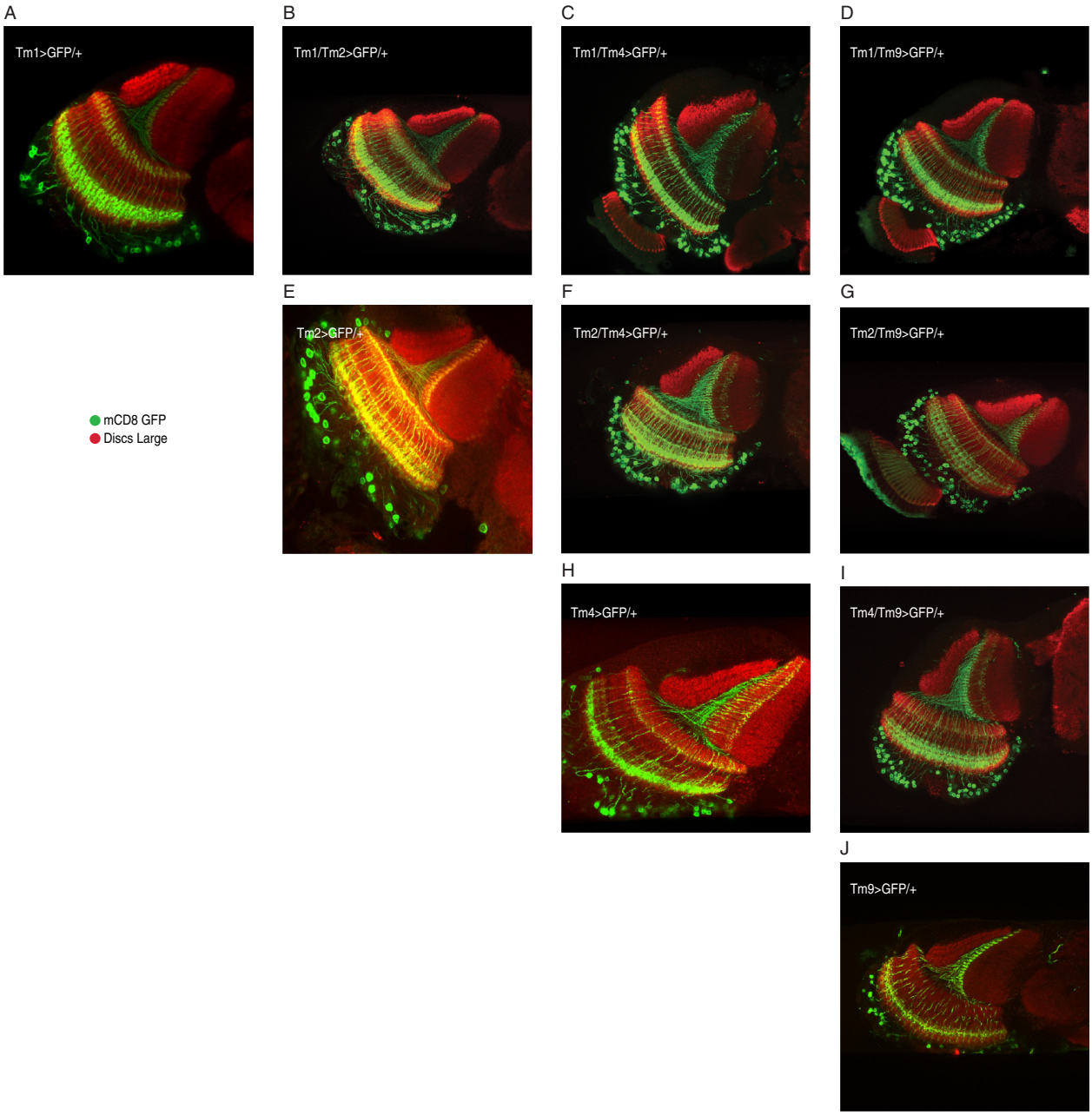

Figure S3. Related to Figures 5-7. Tm cell expression patterns
(A-J) Confocal images of the Gal4 driver cell lines used in the silencing experiments, shown in horizontal cross sections. Tm1 (A), Tm2 (E), Tm4 (H), and Tm9 (J) neurons are labeled in green (mCD8-GFP expression) and neuropils in red (antibody against Discs Large). The six possible binary combinations (B-D, F, G, I) of the Gal4 driver lines exhibit clear expression of two neuron types.

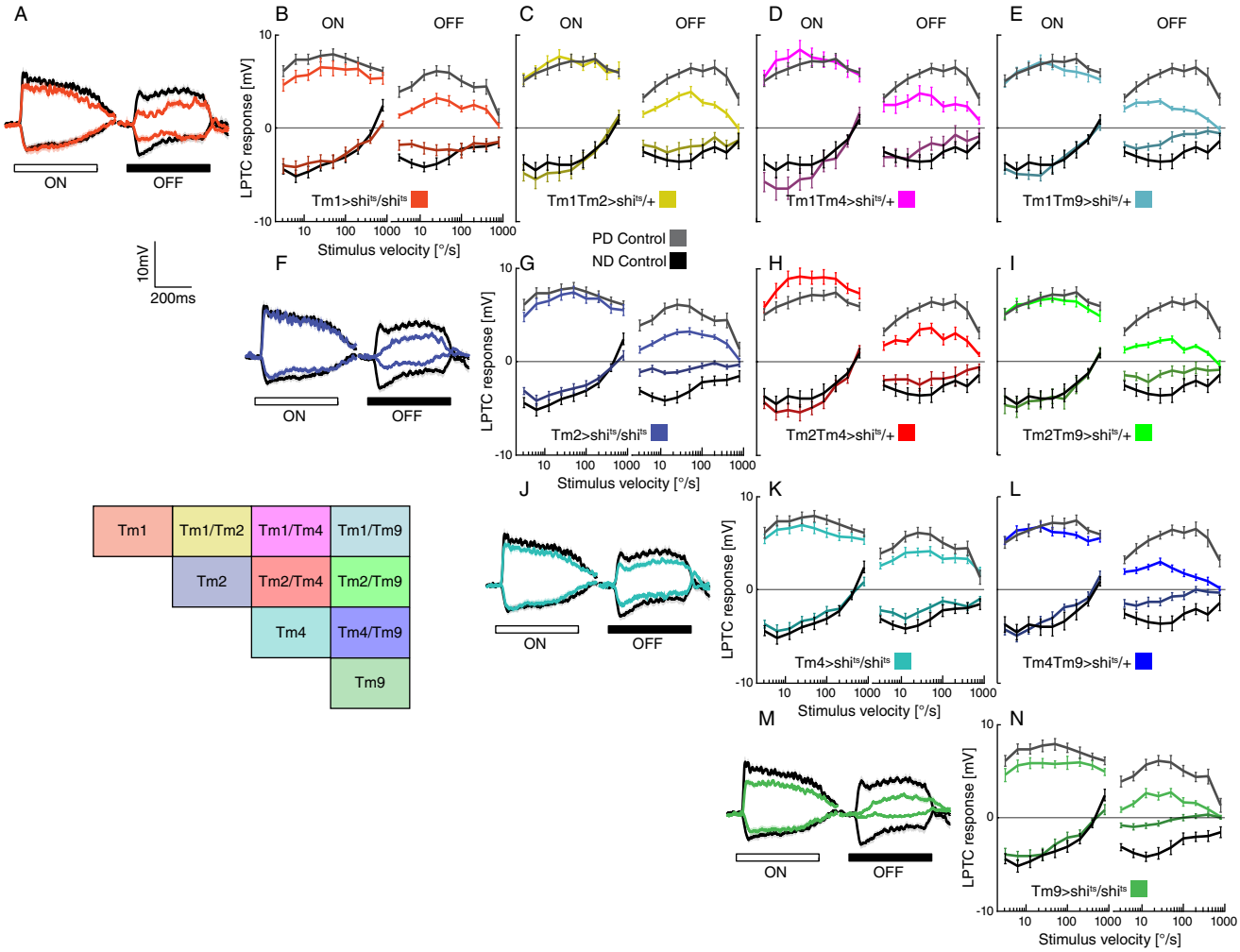

Figure S4. Related to Figures 5 and 6. Preferred and null direction responses of LPTCs to multiple ON and OFF edges
(A, F, J, M) Mean voltage traces of lobula plate tangential cells stimulated with multiple ON and OFF edges moving at 50°/s in preferred (PD) and null direction (ND). Black traces depict recordings from control flies. Red traces in (A) represent LPTC responses in Tm1 block flies, blue traces in (F) Tm2 block flies, cyan traces in (J) Tm4 block flies, and green traces in (M) Tm9 block flies. Error shades indicate ± SEM. (B-E, G-I, K, L, and N) Average responses (errorbars indicate ± SEM) of all four single block (with two copies of shibire^{ts}) and six possible combinations with corresponding controls (black) to multiple ON and OFF edges moving with nine different velocities (3.125˚/s, 6.25˚/s, 12.5˚/s, 25˚/s, 50˚/s, 100˚/s, 200˚/s, 400˚/s, 800˚/s) in PD (light colors) and ND (dark colors). Colored boxes on the bottom left indicate locations of corresponding panels in the matrix.

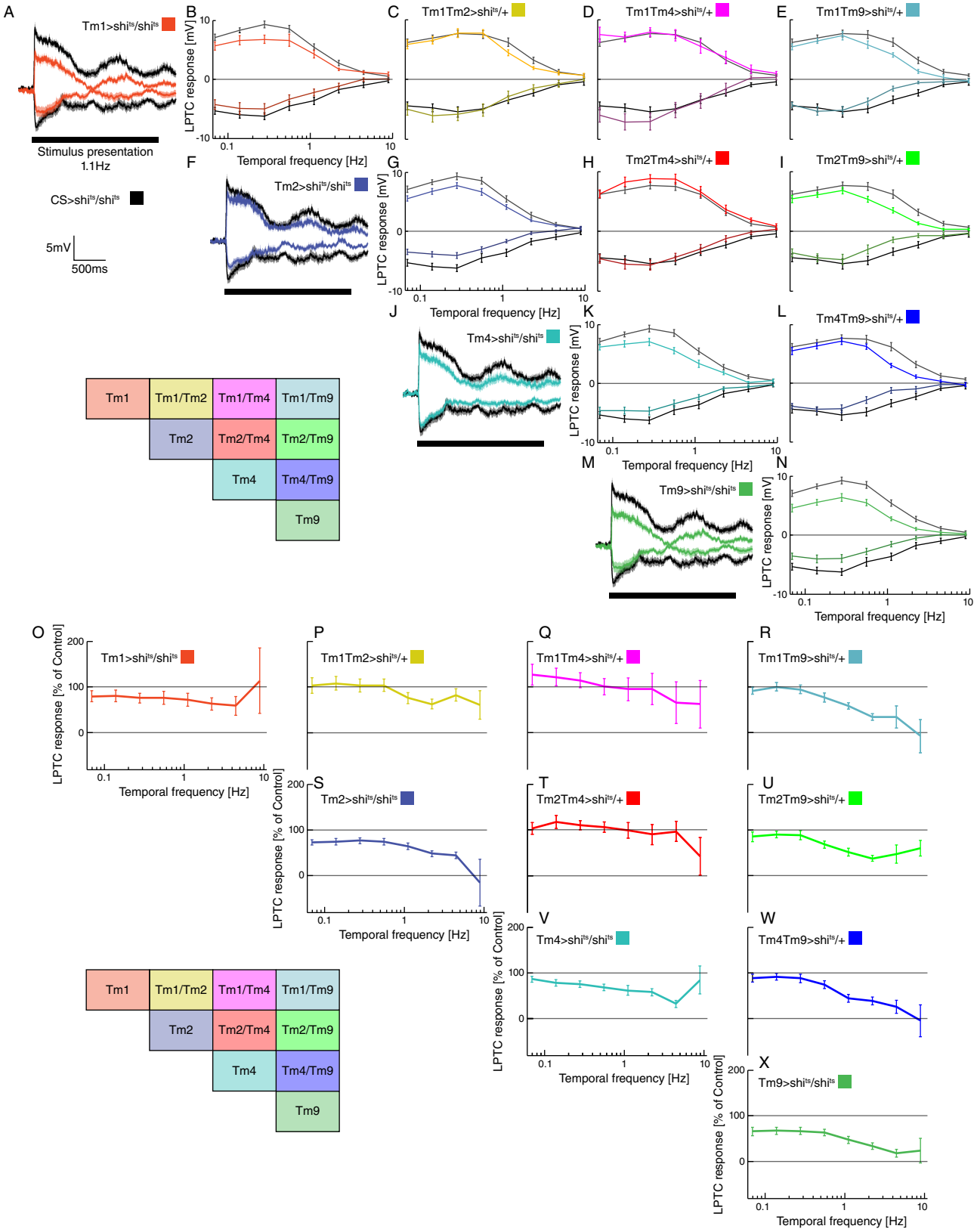

Figure S5. Related to Figures 6 and 8. Detailed analysis of LPTC responses to square wave gratings
(A,F,J,M) Mean voltage traces of lobula plate tangential cells stimulated with square wave gratings (45˚ spatial wavelength) moving at a temporal frequency of 1.11 Hz in preferred (PD) and null-direction (ND). Black traces depict recordings from control flies. Red traces in (A) represent LPTC responses in Tm1 block flies, blue traces in (F) Tm2 block flies, cyan traces in (J) Tm4 block flies, and green traces in (M) Tm9 block flies. Errorshades indicate ± SEM. (B-E, G-I, K,L, and N) Average responses (errorbars indicate ± SEM) of all four single cell block (with two copies of shibire^{ts}) and six possible combinations with corresponding controls (black) to gratings moving with eight different temporal frequencies (0.07Hz, 0.14Hz, 0.28Hz, 0.56Hz, 1.11Hz, 2.22Hz, 4.44Hz, 8.89Hz) in PD (light colors) and ND (dark colors). Colored boxes on the bottom left indicate locations of corresponding panels in the matrix. (O-X) Average voltage responses of LPTCs as above represented as the percentage of the corresponding response in control flies.

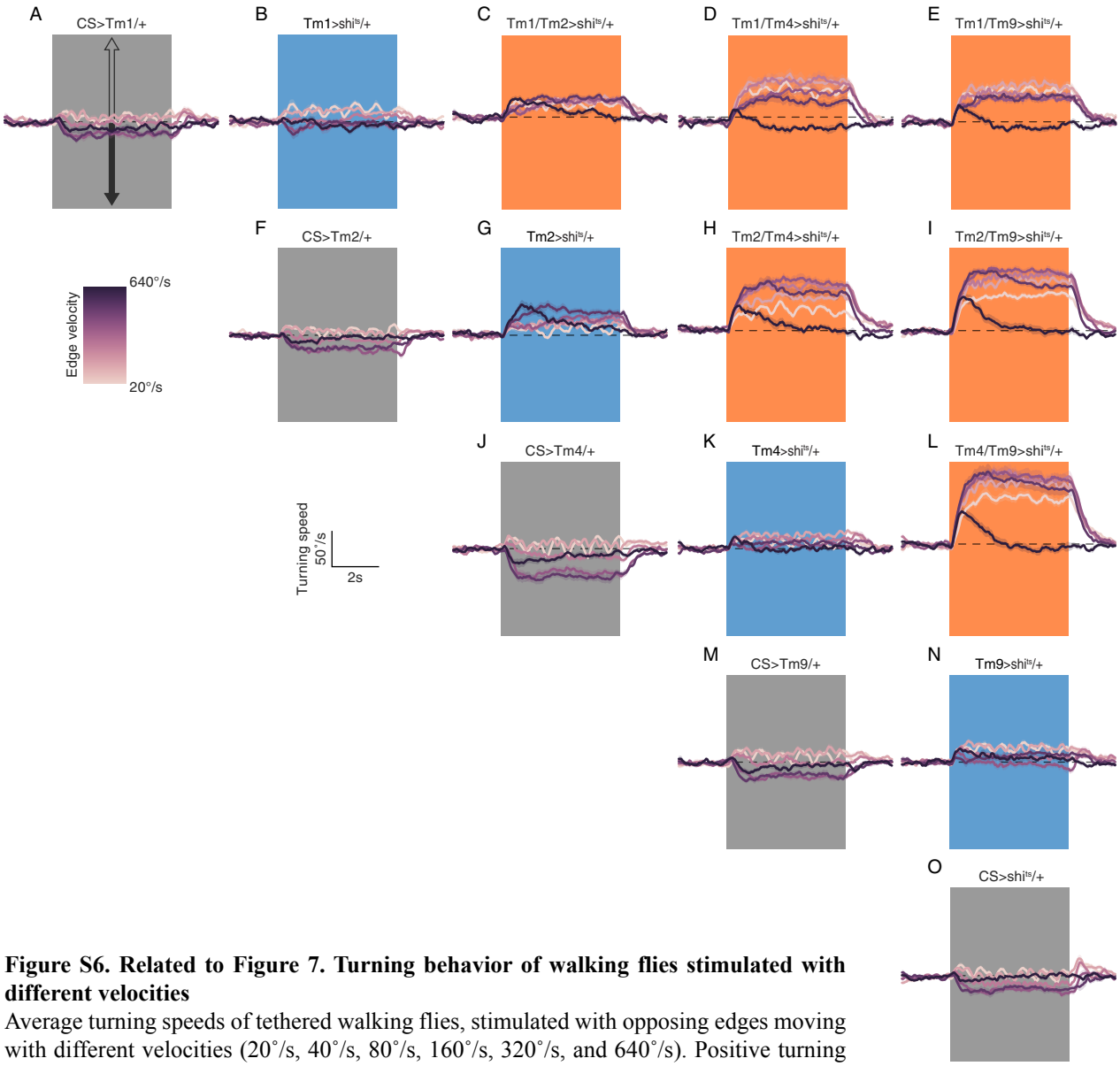

Figure S6. Related to Figure 7. Turning behavior of walking flies stimulated with different velocities

Average turning speeds of tethered walking flies, stimulated with opposing edges moving with different velocities (20˚/s, 40˚/s, 80˚/s, 160˚/s, 320˚/s, and 640˚/s). Positive turning responses correspond to flies turning with ON-edges, negative turning responses indicate turning with OFF-edges (see arrows in A). Stimulus presentation is indicated by shaded boxes. Errorshades indicate ± SEM. (A, F, J, M, and O) Four Gal4 controls and the *shibire^{ts}* control. (B, G, K, and N) Single cell blocks with one copy of *shibire^{ts}*. (C-E, H, I and L) Double cell blocks with one copy of *shibire^{ts}*.

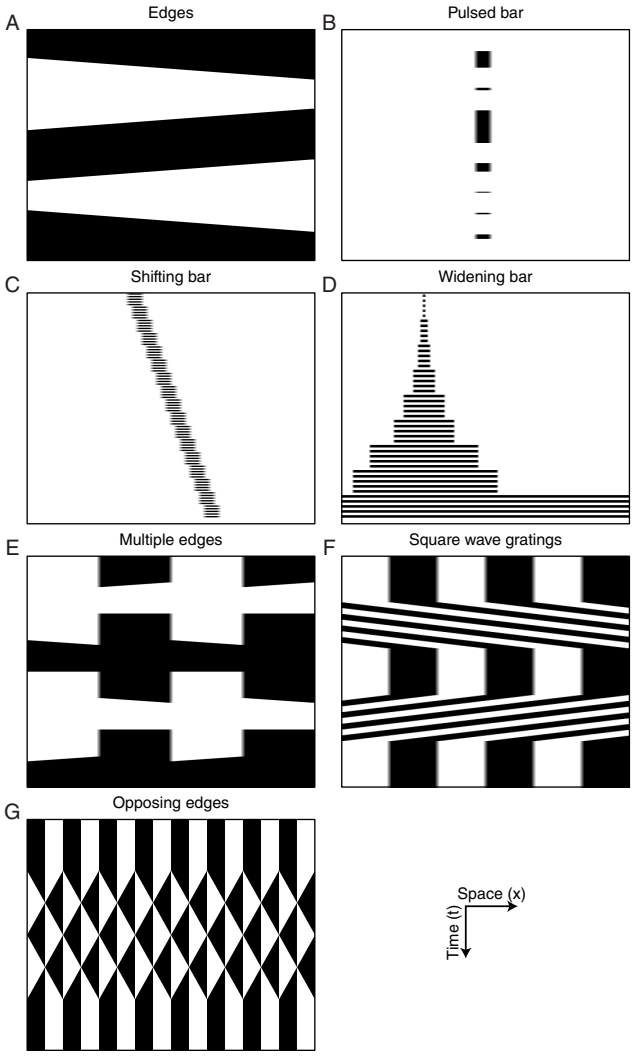

Figure S7. Related to Figures 2-7. Space-time (xt) plots of all visual stimuli used in the study

(A) Single ON and OFF Edges were used for stimulation in Figure 2. (B) Flickering bars with randomly ordered durations were used to test temporal properties in Figure 3. (C and D) Shifting and widening bars were used to test spatial properties in Figure 4. (E) Multiple edges were used in electrophysiological experiments in Figures 5 and 6. (F) Square wave gratings were used in electrophysiological experiments in Figure S5. (G) Opposing edges were used for behavioral experiments in Figure 7.

Movie S1. Related to Figure 4. Retinotopic organization of Tm9 cells

Representative raw two-photon microscope time course of Tm9 cells expressing GCaMP5 (smoothed in ImageJ). The fly is stimulated with a 4.5˚ wide vertical dark bar that is flickering five times at one position and is subsequently shifted by 1.5˚ (see Figure3, Supplemental Experimental Procedures). The movie has been accelerated 8 times (15fps comapred to 1.87Hz acquistion). The insert at the top right indicates the stimulus. Tm9 cell activity follows the stimulus in a retinotopic fashion.

Table S1. Related to Figures 1-7. Genotypes used throughout the study.

Supplemental Experimental Procedures

Flies

Flies were raised on standard cornmeal-agar medium with 12hr light/12hr dark cycles, 25°C, and 60% humidity. Female flies were used for all experiments. For calcium imaging, we used the genetically encoded indicators GCaMP5 (Akerboom et al., 2012) and GCaMP6f (Chen et al., 2013). Blocking experiments were accomplished using Tm cell-specific Gal4 lines crossed with pJFRC100-20XUAS-TTS-Shibire-ts1 (Pfeiffer et al., 2012) flies. Fly line specificity was tested using stochastic flip-out labeling (Nern et al., 2015) and expression of mCD8-GFP. We used different driver lines because of different expression strengths and specificities. All genotypes used in this study can be found in Table S1. Flies were prepared as described previously: imaging experiments, Reiff et al., 2010; electrophysiology, Joesch et al., 2008; and behavior, Bahl et al., 2013.

Immunohistochemistry and confocal imaging

For immuno-staining procedures see Schnell et al., 2010. Primary antibodies used were mouse anti-Discs Large (DLG, RRID:MGI_4354991, Developmental Studies Hybridoma Bank) and anti-GFP-Alexa488 conjugate (RRID:AB_221477, Molecular Probes). For visualization we used (1:200 in PBT): goat anti-mouse Alexa 568 (RRID:AB_10562737). Brains were mounted (Vectashield) and optically sectioned in the horizontal plane with a Leica SP5 confocal microscope. For documentation, single sections were processed in ImageJ 1.46r (NIH, Bethesda, Maryland, USA).

Behavioral experiments

Flies were placed on an air-suspended polyurethane ball in a virtual environment projected onto three monitors spanning approximately 270° (horizontal) and 114° (vertical) of the fly's visual field. This stimulation system offered less than 0.1° of angular pixel size, a value well below *Drosophila's* optical resolution capability. We used six such setups for recording fly locomotion as described previously (Bahl et al., 2013). On two setups, stimuli were presented at a screen refresh frequency of 120Hz; on four setups, the refresh frequency was 144Hz. We never observed qualitative or quantitative differences between these setups in any of the experiments. All monitors were equilibrated in brightness and contrast. Temperature within the immediate surround of the fly was controlled using a custom-built closed-loop thermoregulation system. We employed the following temperature protocol for all experiments and genotypes: Temperature was kept at 25°C for the first 5 minutes and then, within 10 minutes, raised to a restrictive 34°C.

Two-photon microscopy and visual stimulation

Two-photon microscopy and visual stimulus presentation was as described in Maisak et al., 2013. Edges had a contrast of 88%, moving at 30°/s. Each edge motion was shown twice within a single sweep, resulting in a total of eight stimulation periods, each lasting 4s. Subsequent stimuli were preceded by a 3s pause. To map the receptive fields, we flickered 4.5° wide vertical and horizontal dark bars on a bright background with 0.5 Hz at 20 different positions shifted by 1.5°. The position with the maximum response was set to 0°. The responses of the surrounding locations were normalized and plotted dependent on their distance to the peak response. The spatial integration experiments were conducted using vertical dark bars, increasing in size. We measured the responses of flickering bars with 9 different widths (1.5°, 4.5°, 7.5°, 13.5°, 25.5°, 37.5°, 49.5°, 67.5°, 180°) at the peak response position. The responses were normalized to their peak response. For the line scan experiments, a 4.5° vertical dark bar was presented on a bright background for 7 different periods: 50ms, 75ms, 125ms, 225ms, 425ms, 825ms, and 1625ms. The duration of bar presentation was varied in a randomized fashion and each stimulus was presented three times. For the electrophysiology experiments, multiple edges were used as stimuli moving simultaneously at nine different velocities (3.125°/s, 6.25°/s, 12.5°/s, 25°/s, 50°/s, 100°/s, 200°/s, 400°/s, 800°/s). To stimulate HS cells, a vertical, stationary square wave grating with 45° spatial wavelength was presented. For ON edge motion, the right (PD) or the left edge (ND) of each light bar started moving until it merged with the neighboring bar. For OFF edge motion, the right or the left edge of each dark bar was moving. To stimulate VS cells, the pattern was rotated by 90°. Consequently, we used the 36 different stimuli for every recording in a randomized fashion for one to three trials. For behavioral experiments, the balanced motion stimulus resembled previous iterations (Clark et al., 2011). Briefly, we presented flies with a stationary square wave grating that had an initial spatial wavelength of 45° visual angle and a constant Michelson contrast of 50%. Each individual trial lasted 9s. Between 2s and 7s, bright edges moved in one

direction at a fixed velocity while dark edges moved in the other direction at the same velocity. In contrast to previous versions, we reset the stimulus to the initial state after edges had traversed 20° of visual angle. This allowed us to keep the stimulus duration fixed for varying edge velocities. Additionally, we applied a random phase shift after each reset in order to rule out symmetry effects. This was done for 6 velocities (20°/s, 40°/s, 80°/s, 160°/s, 320°/s, and 640°/s) and 2 possible edge directions (dark edge leftwards/bright edge rightwards and vice versa), resulting in 12 conditions that were repeated 50 times per fly. The stimulus was rendered in real-time using Panda3D, an open source game engine, and Python 2.7. x-t plots of all stimuli used are illustrated in Figure S7.

Data analysis and simulations

Data were evaluated off-line using custom written software (Matlab and Python) and Origin (OriginLab Corporation, Massachusetts, USA). To evaluate the calcium imaging data, the raw image series were first converted into a relative fluorescence change (ΔF/F) series by using the first five images as reference. Then, a region was defined within a raw image, and average ΔF/F values were determined within that region for each image, resulting in a ΔF/F signal over time. Example calcium signal traces to edge stimulation were obtained by calculating the average ΔF/F signal over trials. For Figures 2E-2H we normalized the derivative of the mean response trace of every cell. Then, we calculated the mean of the extrema over cells. The evaluation time was the stimulation period with additional four frames.

We fit a three-stage filter model to the mean calcium traces. Within this model, inputs were first high-pass filtered, then rectified by setting negative values to zero, and finally low-pass filtered (Figure 3E). The filters were linear RC filters and of first order. We simulated the visual stimuli as one-dimensional time series whose baseline was zero; for the duration of bar presentation, the values were set to one. The fitting procedure minimized the mean squared error between model output and the calcium traces by exhaustively scanning the two-dimensional parameter space spanned by the time constants of the filters. Errors were summed across presentation lengths of the dark bar, yielding a single optimum per cell type across all seven stimuli. We mapped time constants up to 2000ms in steps of 10ms and additionally allowed filtering to be switched off, equivalent to the time constant being either zero (for a low-pass) or infinite (for a high-pass). The time step for the simulations was 1ms.

To obtain the graphs in Figures 4A-4D and 4F-4I we calculated the mean of the ΔF/F signal of a single axonal arbor of a Tm cell during the time when dark vertical bars were flickering at a certain position for five times and divided that response by the mean of the ΔF/F signal when no stimulation was present. For electrophysiological experiments we calculated the mean over the stimulation time shifted by 25ms. For behavioral experiments we analyzed the data as described previously (Maisak et al., 2013). Briefly, optical tracking sensors were equipped with lens and aperture systems to focus on the sphere behind the fly. The tracking data were processed at 4 kHz internally, read out via a USB interface and processed by a computer at <200 Hz. This allowed real-time calculation of the instantaneous rotation axis of the sphere. We resampled the rotation traces to 20Hz for further processing and applied a first-order low pass filter with a time constant of 100ms to each trace. For all flies, we manually selected 20 consecutive trials out of the 50 available that fulfilled the following criteria: First, the temperature was at a stable 34°C. Second, the average turning tendency of the fly was approximately 0°/s. Third, the average forward velocity of the fly was at least 5mm/s, indicating a visually responsive state. Flies were selected without blinding. Application of the criteria excluded, on average, 20% of all flies. For further processing, we subtracted responses for the two symmetrical edge directions in order to reduce the impact of walking asymmetries. Trials were then averaged. For statistical purposes, we calculated the turning tendency of each fly for each velocity condition as the mean of the turning response between 3s (walking onset) and 7s (stimulus offset). Other evaluation time frames produced qualitatively equivalent results. The scatter plot in Figure 7E was generated by linearly normalizing values to the average of the respective genotype that showed the largest effect and plotting electrophysiology block effects against the natural logarithm of behavioral block effects. We then fit a linear regression model to the transformed data using the least-squares method. All data analysis was performed using Python 2.7 and the NumPy library.

For the modelling results in Figure 8, we simulated grating responses of hypothetical Reichardt detectors whose inputs were bandpass filters as determined in Figure 8. Sinusoidal grating stimuli moved for 3s, preceded and followed by 1s of stationary presentation. The gratings had a spatial wavelength of 10 degrees; no further spatial filtering was applied. An array of 10 detectors viewed the grating. For each possible combination of cells, we then applied the corresponding filters to the two input signals, multiplied the output, and summed over all detectors. This was done twice with spatially mirrored input lines, and results were subtracted and rectified in order to generate an approximation of lobula plate tangential cell signals. Finally, we averaged across the stimulation period. For each cell type combination, we chose the spatial order of input filters such that the mean grating responses were positive. This simulation was performed for 150 temporal frequencies located on a logarithmic scale. Each output was normalized to the maximum response across all cell type combinations.